Conformational Flexibility of Three-Way DNA Junctions Containing Unpaired Nucleotides†

Mengsu Yang‡ and David P. Millar*

Department of Molecular Biology, MB19, The Scripps Research Institute, 10666 North Torrey Pines Road, La Jolla, California 92037

Received December 8, 1995; Revised Manuscript Received April 22, 1996⊗

ABSTRACT: Time-resolved fluorescence resonance energy transfer has been used to examine the global structure and conformational flexibility of three-way DNA junctions containing unpaired bases at the branch point. Three-way junctions were prepared with donor (fluorescein) and acceptor (tetramethylrhodamine) dyes attached to the ends of different helical arms in various pairwise combinations. The time-resolved fluorescence decay of the donor in each labeled junction was measured by time-correlated single photon counting. The distributions of donor−acceptor (D−A) distances present between each pair of labeled helices were recovered from analysis of the donor decay profiles using a Gaussian distribution model. The recovered D−A distance distributions reveal the mean distance between each pair of helices, as well as the range of distances that exists between each pair. For the junction lacking unpaired bases, the three mean interarm distances are similar, indicating an extended structure. In addition, a relatively broad range of distances is present between each pair of helices, showing that the structure is flexible. The addition of unpaired bases causes the junction to fold into a different structure, with one interarm distance being shorter than the other two. The change in overall geometry of the junction appears to be primarily due to the repositioning of one of the helices flanking the bulge. In bulged junctions containing unpaired thymine, cytosine, or adenine bases, the helix containing the 3′ portion of the bulged strand appears to undergo the greatest change in its mean position relative to the other helices. In contrast, in the bulged junction containing unpaired guanine bases, the helix containing the 5′ portion of the bulged strand is displaced. In all bulged junctions, there is a wide range of distances between the perturbed helix and the other two helices, indicating high mobility for the perturbed arm. These results indicate that the overall structure and conformational flexibility of three-way DNA junctions are sensitive to the presence of unpaired bases at the branch point of the junction and that the precise effect of a bulge depends on the nature of the unpaired bases.

Branch points, or junctions, are an important element of nonhelical structure found in many nucleic acids. There is considerable interest in the structure and properties of DNA junctions [reviewed by Lilley and Clegg, (1993) and Seeman and Kallenbach (1994)], primarily because of the role of the four-way Holliday junction in genetic recombination (Holliday, 1964; Messelson & Radding, 1975; Orr-Weaver et al., 1981). Three-way DNA junctions are also of interest, since, as the simplest DNA junctions, they can provide insight into the general principles underlying the folding and stabilization of branched DNA. Moreover, three-way DNA junctions are also involved in certain recombination events (Minigawa et al., 1983; Jensch & Kemper, 1986). In addition to their biological importance and utility as structural models, three-way DNA junctions can also serve as components in nanoconstruction (Liu et al., 1995).

A variety of biophysical and biochemical methods have been employed to probe the structure of three-way DNA junctions. Gel electrophoretic methods have been used to analyze the overall structure of three-way DNA junctions (Duckett & Lilley, 1990; Guo et al., 1990). These studies have shown that the geometry of a three-way DNA junction is dependent on the sequence of bases flanking the branch point as well as those one base pair (bp) removed from the branch point (Lu et al., 1991). Chemical probing experiments with reagents specific for unpaired nucleotides have revealed enhanced reactivity of bases flanking the branch point in a three-way DNA junction (Duckett & Lilley, 1990; Guo et al., 1990). There is evidence from directed ligation studies that the three-way DNA junction has a flexible structure (Ma et al., 1986; Shlyakhtenko et al., 1994a).

Biologically active three-way junctions frequently contain one or more unpaired bases at the branch point of the junction, raising the question of how unpaired bases affect the folding and stability of these species. Leontis et al. (1991) demonstrated that the addition of two unpaired bases to a three-way DNA junction increased its thermodynamic stability. Gel electrophoretic studies of three-way junctions containing added bases at the branch point have shown that the bulged bases alter the overall geometry of the junction (Welch et al., 1993; Zhong et al., 1994). NMR spectroscopy has been used to study the local structure of bulged three-way DNA junctions and to elucidate the conformation of the unpaired bases (Leontis et al., 1994; Rosen & Patel, 1993a,b). A detailed solution structure of a bulged three-way DNA junction has recently been proposed on the basis of two-dimensional NMR data (Ouporov et al., 1994).

† Supported by a grant from the National Science Foundation (MCB-9019250 to D.P.M.).

* Corresponding author.

‡ Present address: City University of Hong Kong, Kowloon, Hong Kong.

⊗ Abstract published in *Advance ACS Abstracts,* June 1, 1996.

S0006-2960(95)02892-3 CCC: $12.00

Enzymatic ligation experiments suggest that bulges also alter the dynamic structure of three-way DNA junctions (Shlyakhtenko et al., 1994b).

Fluorescence resonance energy transfer (FRET)[1] is a useful technique for analyzing the long range structure of nucleic acids (Murchie et al., 1989; Clegg et al., 1992, 1993; Hochstrasser et al., 1992; Eis & Millar, 1993; Tuschl et al., 1994). FRET can be used to determine distances between a donor chromophore (D) and an acceptor chromophore (A) in the 20−80 Å range (Forster, 1949). Due to the relative ease of attachment of suitable fluorophores to synthetic oligonucleotides, there is renewed interest in the application of FRET to structural studies of DNA and RNA. FRET has recently been used to elucidate the overall geometry of four-way DNA junctions (Murchie et al., 1989; Cooper & Hagerman, 1991) and the hammerhead ribozyme (Tuschl et al., 1994) and to observe kinking of DNA and RNA helices by bulged nucleotides (Gohlke et al., 1994). In addition, FRET methods have been employed to investigate DNA hybridization (Cardullo et al., 1988; Morrison & Stols, 1993), to measure thermodynamic and kinetic parameters of DNA triple helix formation (Yang et al., 1994), and to monitor the kinetics of endonuclease-mediated cleavage of DNA (Ghosh et al., 1994).

Most applications of FRET to nucleic acids have been based on steady-state measurements of the integrated emission intensity of the donor or acceptor. Such measurements provide qualitative information on the relative proximity of donor and acceptor probes and can also detect relatively small conformational differences among a series of related molecules. However, time-resolved FRET measurements are more suitable for detailed studies of flexible nucleic acid structures (Eis & Millar, 1993). In time-resolved FRET, the decay of donor fluorescence is measured after picosecond pulse excitation and the decay profile is analyzed with a distance distribution model to obtain information on the mean donor−acceptor distance and the distribution of distances (Haas et al., 1975; Hochstrasser et al., 1992; Parkhurst & Parkhurst, 1995). Time-resolved FRET was recently applied to a four-way DNA junction labeled with donor and acceptor dyes on different helical arms (Eis & Millar, 1993). Very broad distributions of distances were observed between certain pairs of helical arms, reflecting the internal flexibility of the four-way junction in solution.

In the present study, time-resolved FRET is used to examine a series of three-way DNA junctions, both with and without added bases at the branch point of the junction. The aim of these measurements is to assess the impact of unpaired bases on the overall geometry and conformational flexibility of a three-way DNA junction. Fluorescein donors and tetramethylrhodamine acceptors were attached to the ends of various junction arms for measurement of the interarm distances and distance distributions. The three-way junction without added bases is found to adopt an extended structure with a moderate degree of conformational flexibility. Bulged junctions were formed by the addition of two extra thymine, cytosine, adenine, or guanine bases to one junction strand at the point of connection between helices. The distance distributions recovered for the bulged junctions indicate that the unpaired bases perturb the overall structure of the junction. Moreover, the data reveal that unpaired bases have a significant impact on the dynamic structure of the junction, reflected in the high mobility of one of the helices flanking the bulge site. Comparison of the time-resolved FRET data for the different bulged junctions reveals that the effects of bulges on the geometry and flexibility of three-way DNA junctions depend upon the nature of the unpaired bases themselves.

[1] Abbreviations: A, energy transfer acceptor; D, energy transfer donor; F, fluorescein; FRET, fluorescence resonance energy transfer; fwhm, full width of the distribution at half-maximum probability; R, tetramethylrhodamine; R_0, critical transfer distance for donor−acceptor energy transfer; ($\bar{R}$), mean donor−acceptor distance.

MATERIALS AND METHODS

Oligonucleotide Synthesis and Dye Labeling. Oligonucleotides were synthesized on an Applied Biosystems DNA synthesizer (model 108B) using β-cyanoethyl phosphoramidite chemistry. A 5′-aminohexyl group was attached to each oligonucleotide during a final synthesis cycle using aminolink 2 reagent (Applied Biosystems). Donor- and acceptor-labeled DNA strands were prepared by reacting the crude 5′-amino oligonucleotides with succinimidyl ester derivatives (Molecular Probes) of 5-carboxyfluorescein (donor) or 5-carboxytetramethylrhodamine (acceptor) as described (Eis & Millar, 1993). Dye-labeled and unlabeled 5′-amino oligonucleotides were purified by reverse phase HPLC using a gradient of 0.1 M triethylammonium acetate in acetonitrile.

The base sequences of the three oligonucleotides comprising the three-arm junctions are shown in Chart 1. The junction strands are labeled 1−3, while the duplex arms formed by Watson−Crick pairing are labeled by Roman numerals I−III. In the case of bulged three-arm junctions, two additional nucleotides (either guanine, adenine, cytosine, or thymine) were introduced into strand 2 at the point of connection between helices II and III.

Junction Formation. Three-way junctions labeled with only fluorescein (donor-only junctions), or with both fluorescein and tetramethylrhodamine (D−A junctions), were prepared by mixing the appropriate strands in a buffer containing 20 mM Tris, 50 mM NaCl, 5 mM $MgCl_2$, and 0.2 mM EDTA at pH 7.5. In donor-only junctions, the concentration of the donor strand was 0.5 μM and the concentration of the two unlabeled strands was 1.5 μM. The excess of unlabeled strands was used to ensure that all donor strands were bound in three-way junctions. In the D−A junctions, the concentration of donor strands was 0.5 μM and the concentration of the acceptor strand and the unlabeled strand was 1.5 μM. The concentrations of unlabeled and dye-labeled oligonucleotides were estimated by the absorbances at 260, 496 (fluorescein), or 558 nm (tetramethylrhodamine). Dye-labeled junctions are referred to by specifying the dye(s) and labeled strand(s); for example, F1 refers to a singly labeled junction in which fluorescein is attached to strand 1, while F1R2 refers to a doubly labeled junction in which fluorescein is attached to strand 1 and tetramethylrhodamine is attached to strand 2. The DNA strands were annealed into junctions by heating the solutions at 80 °C for 5 min and then slowly cooling to room temperature.

Time-Resolved Fluorescence Measurements. The time-resolved decay of fluorescein emission following pulsed

Chart 1. Three-Way DNA Junctions Examined in the Present Study[a]

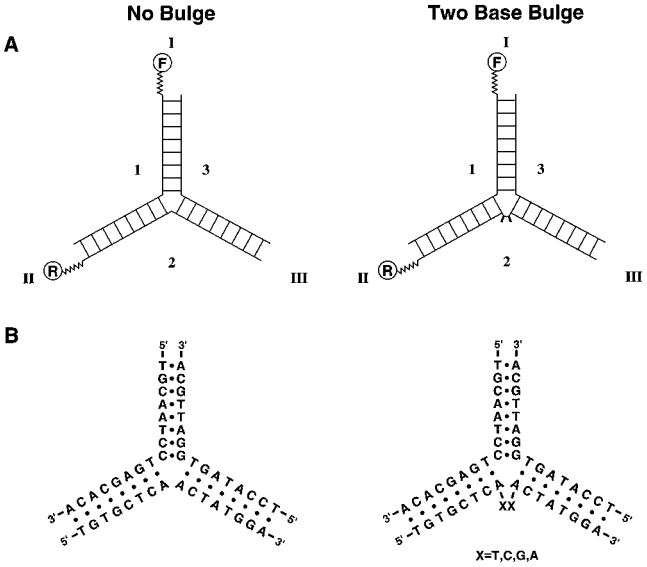

[a] (A) Schematic representation of dye-labeled three-way junctions without added bases (left-hand side) and with two added bases in one strand (right-hand side). Junction strands are labeled 1−3. Duplex arms formed by Watson−Crick pairing are labeled I−III. For FRET measurements, two strands are labeled at their 5′ ends with either fluorescein (donor) or tetramethylrhodamine (acceptor) dyes. In the particular example shown here, strand 1 is labeled with fluorescein and strand 2 is labeled with tetramethylrhodamine. The resulting labeled junction is denoted F1R2. Other labeled junctions were also prepared for measurement of the three interarm distances and distance distributions in the three-way junction. These have fluorescein attached to strand 1 and tetramethylrhodamine attached to strand 3 (denoted F1R3) or fluorescein attached to strand 2 and tetramethylrhodamine attached to strand 3 (denoted F2R3). (B) Sequences of three-way junctions without added bases (left-hand side) or with various added bases in strand 2 (right-hand side). In the right-hand diagram, the two extra bases introduce a two-base bulge at the branch point of the junction. Bulged junctions were prepared in which either two unpaired thymine, cytosine, adenine, or guanine bases were added to strand 2.

excitation was measured in donor-only and D−A junctions using the time-correlated single photon counting system described in detail elesewhere (Eis & Millar, 1993). Fluorescein was repetitively excited at 514.5 nm with 90 ps duration pulses from a mode-locked argon ion laser (Coherent Innova 100−12). An external pulse selector reduced the pulse repetition frequency from 78 to 3.08 MHz. Fluorescence was collected at 90° to the excitation beam, passed through a polarizer oriented at 54.7° to the vertical excitation polarization, and focused onto the entrance slit of a 0.1 m single grating monochromator (JY H-10). Fluorescein emission was monitored at 530 nm. Fluorescence was detected using a microchannel plate photomultiplier (Hamamatsu R2809U-01), whose output was processed with time-correlated single photon counting electronics. Decay curves were collected in a multichannel analyzer (Ortec-Norland, model 5510) until at least 10 000 single photon counts had been accumulated in the peak channel. The instrument response function (fwhm = 100 ps) was measured using a dilute solution of nondairy coffee creamer to scatter the laser pulses into the detector. All measurements were performed at 20 °C.

Data Analysis. The intrinsic fluorescence lifetimes of the fluorescein donor were determined by analysis of the fluorescence decay of donor-only junctions. Donor-only decays were analyzed by fitting to a sum of exponential functions,

$$I_D(t) = g(t) \otimes K(t) \quad (1)$$

and

$$K(t) = \sum_{i=1}^{N} \alpha_i \exp(-t/\tau_i) \quad (2)$$

where $I_D(t)$ is the isotropic fluorescence intensity of the donor-only junction at time t after excitation, $g(t)$ is the instrument response function, ⊗ denotes convolution of two functions, α_i is the fractional amplitude associated with each donor lifetime τ_i, and N is the number of lifetimes. The method of nonlinear least squares (Bevington, 1969) was used to adjust the parameters α_i and τ_i to obtain a best fit. The goodness of fit was judged by the reduced chi-square value, χ_R^2, and by examination of the weighted residuals.

The fluorescence decay of the donor in D−A junctions, $I_{DA}(t)$, was analyzed according to eq 3

$$I_{DA}(t) = g(t) \otimes [(1 - f)\int_{R_{min}}^{R_{max}} \sum_i \alpha_i \exp\{(-t/\tau_i)[1 + (R_0/R)^6]\} P(R)\, dR] + fI_D(t) \quad (3)$$

wherein the probability distribution of D−A distances, $P(R)$, is assumed to be static on the time scale at which energy transfer occurs, R_0 is the critical transfer distance for energy transfer from fluorescein to tetramethylrhodamine (54.3 Å; Eis & Millar, 1993), R_{min} is the distance of closest approach of the donor and acceptor, and R_{max} is the maximum D−A distance. R_{min} and R_{max} were set to 3 and 100 Å, respectively. The *intrinsic* donor lifetimes τ_i and amplitudes α_i were obtained from the decay of donor-only junctions, as described above. The expression in square brackets in eq 3 represents the idealized decay of a single donor−acceptor configuration, averaged over the probability distribution of all D−A distances. Equation 3 also contains a correction term to account for a fraction (f) of donors that do not undergo energy transfer because of incomplete junction formation.

The D−A distance distribution was described by a weighted Gaussian distribution of distances (Haas et al., 1975):

$$\begin{aligned} P(R) &= c4\pi R^2 \exp[-a(R-b)^2] \quad \text{for } R_{min} < R < R_{max} \\ &= 0 \quad \text{elsewhere} \end{aligned} \quad (4)$$

where a and b are adjustable parameters and c is a normalization constant.

Equation 3 was used to fit the fluorescein decay in each D−A junction by optimizing the parameters a and b in eq 4, as well as the fraction of free donor species (f). The intrinsic donor lifetimes were kept constant in the analysis of the D−A junctions. The quality of the fit was assessed as described above. The D−A distance distributions corresponding to the best fit of the donor decay were calculated from eq 4 using the fitted values of a and b. The distributions were normalized to unit area. The mean D−A distance ($\bar{R}$) was evaluated as the first moment of the recovered distribution. The full width of the distribution at half maximum probability (fwhm) was also evaluated.

The donor decays in D−A junctions were also analyzed under the assumption that a single D−A distance is present.

In this case, the integral in eq 3 was replaced by a single term in which the exponent is evaluated at only one D−A distance. The donor decays were fitted by optimizing this distance. The donor decays were also fitted with a model based on two discrete D−A distances. For this model, the integral in eq 3 was replaced by a sum of two terms, with relative weights p_1 and p_2, and distances R_1 or R_2 appearing in the exponent of each term. The donor decays were fitted by optimizing the two distances and their relative weights for the best fit (it was only necessary to vary p_1 since the value of p_2 is determined by the requirement that $p_1 + p_2 = 1$). The fits based on a single D−A distance, or two discrete D−A distances, were compared with corresponding fits obtained using a Gaussian distribution of D−A distances.

RESULTS

Formation of Three-Way Junctions. Since all FRET measurements are based on the fluorescence decay of the donor, it is important to ensure that all donor-labeled strands are present in three-way junction complexes. To do this, a given donor strand was titrated with increasing amounts of the complementary acceptor-labeled and unlabeled strands, until there was no further change in the fraction of free donor strands. Free and bound donor strands were distinguished on the basis of their different fluorescence decay behavior, since free donor strands do not undergo energy transfer to an acceptor. Fluorescence decay curves were analyzed according to eq 3, which contains separate terms for free and bound donor strands, yielding an estimate of the fraction of free donor strands present at each point in the titration. This method was previously used to monitor formation of four-way DNA junctions labeled with the same dye pair as used here (Eis & Millar, 1993). A progressive reduction in the fraction of free donor strands was observed as increasing amounts of the complementary acceptor-labeled and unlabeled strands were added, reflecting the formation of three-way junctions. In a typical case, the fraction of free donor strands reached a limiting value close to zero after approximately one stoichiometric equivalent of the acceptor-labeled and unlabeled strands had been added to the donor strand. These results indicate that energy transfer from fluorescein to tetramethylrhodamine is occurring within a complex comprised of one donor strand, one acceptor strand and one unlabeled strand. In order to minimize the fraction of free donor strands, all junction samples used in subsequent FRET measurements were prepared with a 3-fold excess of acceptor-labeled and unlabeled strands relative to the donor strand. It should be noted that the presence of excess acceptor-labeled and unlabeled strands does not complicate the interpretation of the FRET data, since only the donor-labeled strands are observed in the fluorescence decay measurements.

Conformational Analysis of a Perfect Three-Way Junction. The overall geometry of the three-way DNA junction without added bases was analyzed by means of FRET between donor and acceptor dyes attached to the ends of the helical arms. The sequence of the perfect three-way junction is shown in Chart 1. Junctions were constructed with a fluorescein donor attached to the 5′ end of one strand and a tetramethylrhodamine acceptor attached to the 5′ end of another strand. FRET analysis of three doubly labeled constructs is sufficient to define the overall geometry of the three-way junction. These are denoted F1R2, F1R3, and F2R3, where, for example, F1R2 indicates that strand 1 is 5′-labeled with fluorescein and strand 2 is 5′-labeled with tetramethylrhodamine (see Chart 1). Junctions were also constructed with only the fluorescein donor, attached to either strand 1 or strand 2 (donor-only junctions F1 and F2, respectively), for measurement of the intrinsic donor lifetimes.

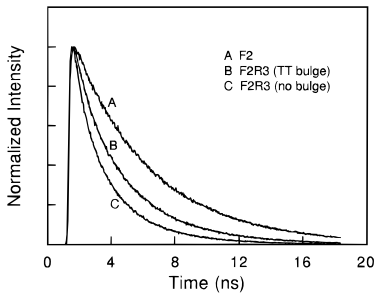

FIGURE 1: Fluorescence decay profiles of fluorescein donors attached to three-way DNA junctions. Fluorescein was excited at 514.5 nm, and the emission was detected at 530 nm. Measurements were performed at 20 °C. (A) Decay of donor-only junction F2 (fluorescein attached to strand 2, strands 1 and 3 unlabeled). (B) Decay of D−A junction F2R3 (fluorescein attached to strand 2, tetramethylrhodamine attached to strand 3, strand 1 unlabeled) with two added thymine bases in strand 2 (see Chart 1 for the sequence of strand 2 in the bulged junction). The decay is slower than in the junction without added bases (C), indicating that the distance between helices II and III is larger in the presence of the extra thymine bases. (C) Decay of D−A junction F2R3 without added bases. The faster decay of fluorescence compared to that in curve A reflects energy transfer from fluorescein to tetramethylrhodamine. The D−A distributions recovered by analysis of the donor decays shown in curves B and C are depicted in Figure 2 (lower panel).

The intrinsic fluorescence lifetimes of the donor at each labeled position were determined in the donor-only junctions F1 and F2. The fluorescence decay of fluorescein was fitted to a sum of exponentials, according to eqs 1 and 2. In each case, the best fit was obtained with two decay components (typical χ_R^2 values are between 1.05 and 1.25). The parameters describing the intrinsic fluorescence decay of fluorescein attached at the end of helix I are as follows: $\tau_1 = 1.2$ ns ($\alpha_1 = 0.09$) and $\tau_2 = 5.1$ ns ($\alpha_2 = 0.91$). Similar values were obtained for fluorescein attached to helix II. The long decay time, which accounts for most of the decay amplitude, is similar to the lifetime of free fluorescein under similar solution conditions. The observation of a second, shorter decay time indicates that fluorescein is partially quenched, possibly as a result of dye−DNA interactions. However, on the basis of the relative weights of the two decay times, it is apparent that the quenching only affects a very small population (9%) of the linked dyes. These results indicate that the fluorescein donor experiences a predominantly aqueous environment and does not interact with the DNA structure to any significant extent. This was also confirmed by time-resolved anisotropy measurements (see below). These results are in accord with time-resolved fluorescence data previously obtained for fluorescein attached to a four-way DNA junction using the same six-carbon linker and with the same base sequence at the point of dye attachment as used here (Eis & Millar, 1993).

Fluorescence decays of the fluorescein donor were measured in the three D−A-labeled junction constructs for calculation of the three interarm distances and distance distributions in the three-way junction. Energy transfer from fluorescein to tetramethylrhodamine is manifested as a more rapid decay of the donor fluorescence (Figure 1). We first tried to fit the donor decays by assuming that a single D−A

distance is present in each doubly labeled junction. The distance was optimized using nonlinear least squares fitting. However, the resulting fits were very poor in all three D−A junctions, reflected in large systematic deviations (not shown) and unacceptable χ_R^2 values (14−23). We next tried to fit the donor decays assuming that two discrete D−A distances are present in each doubly labeled construct. The two distances and their relative weights were optimized to fit the donor decay profiles. Reasonable fits were obtained for the F1R2 and F1R3 species ($\chi_R^2 = 1.3-1.5$), but the donor decay in F2R3 was not described well in terms of two discrete D−A distances ($\chi_R^2 = 1.8$). The donor decays were then analyzed assuming that the distance between donors and acceptors is described by a Gaussian probability distribution (eq 4). The decay profiles were fitted by adjusting the distribution parameters *a* and *b*, which yielded excellent fits to all three doubly labeled species ($\chi_R^2 = 1.2-1.3$). These results indicate that the distance distribution model provides an equivalent or better description of the donor decay profiles than does the model of two discrete distances, despite having one less adjustable parameter. Since the distribution model can account for all the donor decays using the smallest number of adjustable parameters, we concluded that the interarm distances in the perfect three-way junction are best described as distributions.

In the fits to the various models decribed above, the correction term for free donor strands was not included in any of the analyses. This was necessary because variations in this term could compensate for differences between the various models and thereby complicate the comparisons. Having established that the distance distribution model was appropriate, we subsequently reanalyzed the donor decays for the three doubly labeled species by including the correction term for free donor strands (second term in eq 3), even though these species were expected to be negligible. The fraction of free donors was freely optimized in this second round of fitting, which resulted in a small improvement in the fits. The data reported later in Figure 2 and Table 1 refer to the results of these fits. The fractions of free donor strands recovered from these fits are indeed very small (Table 1), confirming that complete junction formation was achieved in each of the three doubly labeled samples.

The D−A distance distributions corresponding to the best fit of the donor decays were calculated from eq 4 using the fitted values of *a* and *b*. The recovered distributions are shown in Figure 2 for the F1R2, F1R3, and F2R3 junctions. The mean D−A distances and distribution widths are summarized in Table 1. These results indicate that two of the interarm distances in the three-way junction are very similar (between helices I and III, and between helices II and III), whereas the third distance is slightly larger (between helices I and II). Thus, the overall structure of the perfect junction appears to be somewhat asymmetric. Heterogeneity in the junction structure is reflected in the widths of the interarm distance distributions. The full width of the distribution at half-maximum probability reflects the range of distances between the 5′ ends of the labeled strands as reported by the donor and acceptor dyes. The distributions are broader than expected simply on the basis of the flexibility of the linkages used to attach the donor and acceptor dyes to the junction arms. This can be appreciated by comparing the distributions for the three-way junction with similar data obtained for a short DNA duplex labeled at opposite ends with the same dye and linker combinations as used here. Time-resolved FRET analysis of the labeled duplex revealed a D−A distribution with a full width at half-maximum of 12 Å (Hochstrasser et al., 1992), which presumably reflects the intrinsic flexibility of the six-carbon

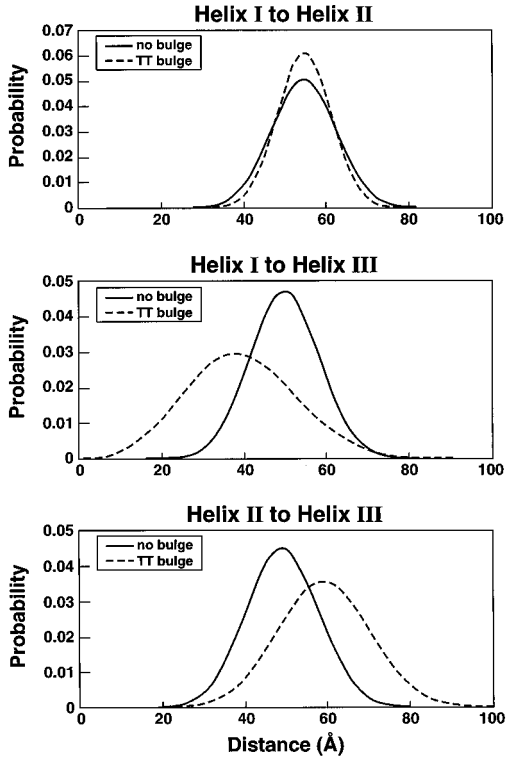

FIGURE 2: Interarm distance distributions in three-way DNA junctions. Distributions were recovered from analysis of donor decay profiles according to eqs 3 and 4. Distributions are shown for a three-way junction without added bases (solid lines) and for the corresponding junction with two extra thymine bases in strand 2 (dashed lines). Distributions are shown for each of the interhelical distances in the three-way junction.

Table 1: Donor−Acceptor Distances in Dye-Labeled Three-Way Junctions

labeled strands[a]	$\bar{R}$ (Å)[b]	fwhm (Å)[c]	f[d]
Perfect Junction			
F1R2	54.8	18.7	0.070
F1R3	50.1	20.0	0.046
F2R3	49.3	21.0	0.018
TT Bulge			
F1R2	55.0	15.4	0.036
F1R3	39.8	32.4	0.006
F2R3	59.3	26.5	0.034
CC Bulge			
F1R2	56.5	18.0	0.212
F1R3	40.6	28.6	0.022
F2R3	57.8	26.6	0.001
AA Bulge			
F1R2	54.5	19.3	0.049
F1R3	45.0	36.4	0.028
F2R3	62.6	45.1	0.181
GG Bulge			
F1R2	51.8	31.1	0.102
F1R3	50.2	22.3	0.022
F2R3	56.5	38.2	0.200

[a] F*m*R*n* denotes that strands *m* and *n* are labeled at their 5′ termini with fluorescein and tetramethylrhodamine, respectively. Junction samples contained a 3-fold molar excess of acceptor-labeled and unlabeled strands compared to the donor-labeled strand. [b] Mean D−A distance, calculated as the first moment of the recovered D−A distance distribution. [c] Full width of the D−A distance distribution at half-maximum probability. [d] Fraction of free donor strands.

linkers since the short DNA duplex is expected to be rigid. The interarm distance distributions in the three-way junction are all considerably broader than 12 Å (Table 1). This indicates that a range of distances exists between each pair of helices in the three-way junction. Moreover, the distance heterogeneity appears to be similar between each pair of junction arms (Table 1).

The present analysis of the donor decays does not include orientational effects on energy transfer. Fluorescence anisotropy decay measurements of junctions labeled with only fluorescein or tetramethylrhodamine (not shown) indicate that both dyes enjoy considerable rotational freedom when attached to the ends of the junction arms by six-carbon linkers. Rapid local rotation of the dyes was reflected in an initial subnanosecond decay of anisotropy, measured at 530 nm (fluorescein) or 580 nm (tetramethyrhodamine). The amplitude and correlation time describing the local rotation of the dyes were essentially identical to those reported previously for the same dyes attached to a four-way DNA junction (Eis & Millar, 1993). The amplitude of motion was large for both dyes (cone semiangles in the 35−40° range) and was independent of the labeling position. Such rapid motions of the donor and acceptor result in almost complete dynamic averaging of the orientation factor for energy transfer. We have previously shown that the D−A distance distributions recovered under these conditions are not biased by orientational effects on energy transfer (Eis & Millar, 1993).

Previous FRET studies employing fluorescein and tetramethylrhodamine dyes attached to DNA or RNA have also reported high mobility for fluorescein but have indicated considerably less rotational freedom for tetramethylrhodamine (Clegg et al., 1992; Tuschl et al., 1994). The lower rotational mobility of tetramethylrhodamine observed in these studies may reflect a greater tendency of the dye to interact with the surrounding DNA or RNA structure. Previous studies have shown that the fluorescence lifetime properties of dyes attached to DNA are highly dependent upon the base sequence adjacent to the point of dye attachment (Millar et al., 1992), presumably due to specific dye−DNA interactions. It is likely that the rotational properties of DNA- or RNA-linked dyes may also be dependent upon the base sequence near the point of attachment. We note that the 5′-terminal sequences of the oligonucleotides employed in the present study were chosen on the basis of previous studies showing that dye−DNA interactions are minimized by attachment of dyes to DNA via 5′ thymidine residues (Millar et al., 1992; Eis et al., 1993).

Geometry and Flexibility of Bulged Three-Way DNA Junctions. The effect of unpaired nucleotides on the overall geometry and flexibility of the three-way junction was examined by introducing two unpaired nucleotides into strand 2 at the point of connection between helices II and III, resulting in a two base bulge at the branch point of the junction (Chart 1). Bulged junctions containing two unpaired thymine, cytosine, adenine, or guanine bases were examined by time-resolved FRET. Apart from the added bases, the three-way junctions are otherwise identical.

Figure 1 shows the effect of two unpaired thymine bases on the fluorescence decay of the fluorescein donor in the F2R3 junction. Clearly, the extent of donor quenching is reduced in comparison with that of the perfect junction, indicating that the addition of two thymines at the branch point of the junction increases the distance between helices II and III. The donor decay profiles were measured for each D−A labeled junction species and analyzed using either the distance distribution model or a model of two discrete D−A distances (the free donor term was excluded in both analyses, as descibed earlier). Excellent fits were obtained for all three doubly labeled species using the distribution model ($\chi_R^2 = 1.1-1.4$). The discrete model yielded less satisfactory fits, especially in the case of the F1R3 species ($\chi_R^2 = 4.1$). The data were therefore subsequently interpreted in terms of a distribution of distances. Similar conclusions were drawn for the other bulged junctions presented later. Inclusion of the free donor term in a second round of fitting the decays for the TT-bulged junction revealed that the fraction of free donor strands in each doubly labeled sample was very small (Table 1), showing that the addition of two thymines to strand 2 did not interfere with junction formation. The data presented in Figure 2 and Table 1 were obtained during this second round of fitting.

The recovered interarm distance distributions for the TT-bulged junction are compared with the same distributions for the perfect junction in Figure 2. It is immediately apparent that the addition of unpaired thymines results in a shorter distance between helices I and III, and a correspondingly larger distance between helices II and III. This is also reflected in the mean interarm distances reported in Table 1. In addition, the corresponding distance distributions are much broader in the bulged junctions (Figure 2 and Table 1). In contrast, the thymine bulge has little effect on the mean distance between helices I and II or on the range of distances between these helices. The simplest interpretation of these data is that helix III moves to a new position in the bulged junction, while the mean positions of helices I and II remain relatively fixed (Figure 4). Moreover, since the distance distributions measured from helix III to either of the other helices are much broader in the bulged junction, while the helix I to helix II distribution is unaffected by bulges, it appears that helix III can occupy a wider range of positions in the bulged junction.

The results obtained for the junctions containing cytosine or adenine bulges are similar to those for the thymine-bulged junction. In each case, it appears that helix III is specifically perturbed by the bulged bases, while the separation of helices I and II is hardly affected (Table 1). Moreover, the interarm distance distributions in these bulged junctions reveal a similar pattern of broadening relative to the perfect junction, again indicating that helix III has greater mobility (Table 1). In certain instances, the fraction of free donor strands is larger in the AA-bulged and CC-bulged junctions than in the junction without added bases (Table 1). This may indicate that the bulged cytosines or adenines can interfere to some extent with junction formation. In fact, since a larger fraction of free donor strands is observed for either the F1R2 or F2R3 species (Table 1), it appears that pairing of strand 2 with either strand 1 or strand 3 may be perturbed by the bulges. This is not surprising given that strand 2 contains the extra adenine or cytosine bases. It is important to note that the presence of free donor strands does not bias the distance parameters obtained for the intact junction complex, because the free donor strands are explicitly accounted for in the analysis (Eis & Millar, 1993).

The presence of two unpaired guanine bases at the branch point of the three-way junction has a qualitatively different effect on the overall structure and flexibility of the complex than do the other bulges (Figure 3 and Table 1). The distance distribution between helices I and III is hardly affected by

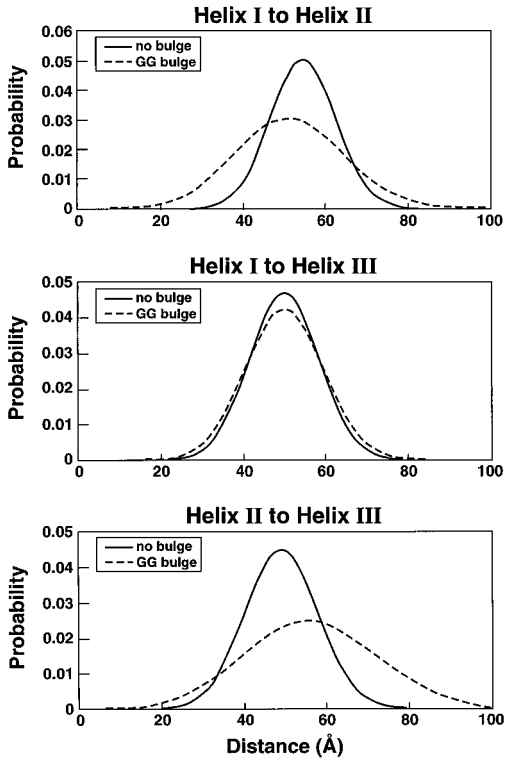

FIGURE 3: Effect of unpaired guanines on the distribution of distances between each pair of helices in the three-way DNA junction. Interarm distributions in the junction without added bases (solid lines) are compared with corresponding distributions for the junction with two extra guanine bases in strand 2 (dashed lines).

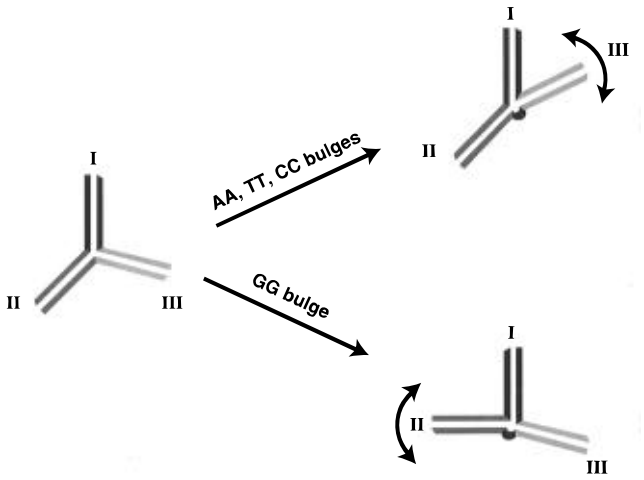

FIGURE 4: Schematic interpretation of the results from distance distribution analysis of three-way DNA junctions with and without added bases. The overall structure of the junction without added bases is somewhat asymmetric, with the I−II distance being larger than the other two interarm distances. Addition of two extra thymine, cytosine, or adenine bases at the branch point of the junction causes helix III to move closer to helix I and further away from helix II, while having little effect on the distance between helices I and II. Moreover, helix III has greater mobility in the bulged junctions and can sample a wide range of positions, indicated by the curved arrow. In contrast, addition of two extra guanines to the three-way junction displaces helix II, causing it to move closer to helix I, while having no effect on the distance between helices I and III. In addition, helix II has greater mobility in the bulged junction, again indicated by the curved arrow.

the unpaired guanines, while the distance between helices I and II is somewhat reduced, and the distance between helices II and III is greater than in the perfect junction. In addition, the range of distances between helix II and each of the other two helices is considerably broader in the bulged junction (Table 1). These data suggest that the GG bulge perturbs the equilibrium position of helix II, while also increasing its mobility with respect to the other arms, but has little effect on the spatial relationship between helices I and III (Figure 4). However, the changes in the interarm distances are less pronounced than observed for the other types of bulges. In addition, in the case of F1R2 and F2R3, the fraction of free donor species is larger than in the perfect junction (Table 1). This suggests that strand 2 may not bind as well with the other junction strands when the extra guanine bases are present, which is similar to the effects noted above for bulged cytosines or adenines.

DISCUSSION

The goal of the present study is to characterize the effects of bulged nucleotides on the overall structure and conformational flexibility of a three-way DNA junction. To this end, we have synthesized junctions containing fluorescent donor and acceptor groups conjugated to the ends of the helical arms for measurements of fluorescence resonance energy transfer. By measuring FRET in a set of doubly labeled DNA molecules in which each pair of helices are labeled in turn, we have been able to define the overall spatial arrangement of the three junction arms. We have chosen to adopt a time-resolved FRET methodology, based on analysis of the fluorescence decay of the donor, because this approach is very sensitive to molecular flexibility. An earlier study of a four-way DNA employing time-resolved FRET revealed a considerable degree of flexibility in the overall structure of the junction, and we anticipated that three-way DNA junctions might also be flexible. We were particularly interested in the effect that bulged nucleotides would have on the overall conformational flexibility of the three-way junction. Apart from the question of conformational flexibility, another reason for the choice of time-resolved FRET measurements is the ability to accurately report the mean interarm distances, even when there is considerable dispersion in these distances. In contrast, steady-state measurements of FRET overestimate the mean D−A distances when a broad distribution of distances is present, as shown in the study of a four-way DNA junction (Eis & Millar, 1993). The mean interarm distances in the three-way junction must be accurately determined since these define the overall geometry of the complex.

We first examined a three-way junction without any added bases, in order to provide a benchmark for comparison with junctions containing bulged bases. In the junction without added bases, two of the mean interarm distances are approximately equal, while the third distance is somewhat larger than the other two (Table 1). These results indicate that the three-way junction without added bases adopts an extended and somewhat asymmetric structure. This is consistent with earlier studies in which gel electrophoretic methods were used to analyze the overall geometry of three-way DNA junctions. These studies have shown that a perfect three-way DNA junction adopts an asymmetric structure in which two branch angles are similar, while the third angle is more obtuse (Guo et al., 1990).

Bulged three-way junctions were formed by the addition of two unpaired nucleotides to strand 2, at the point of connection between helices II and III. The bulge composition was varied by adding either two thymine, cytosine, adenine, or guanine bases to strand 2 (Chart 1). The FRET data reveal that the overall structure of the bulged junctions

is markedly asymmetric, with one of the interarm distances being shorter than the other two. This is consistent with gel electrophoretic studies of bulged three-way DNA junctions, which show that one of the branch angles in the junction becomes more acute following the addition of unpaired bases at the branch point (Zhong et al., 1994). Moreover, the FRET data provide insight into the nature of the structural rearrangements of the three-way junction that are necessary to accommodate the extra bases at the branch point of the junction and show how these rearrangements depend on the nature of the unpaired bases themselves. Comparison of the mean interarm distances in the perfect and bulged junctions reveals that the change in global topology due to bulges is primarily due to the repositioning of one of the helices flanking the bulge. In bulged junctions containing unpaired thymine, cytosine, or adenine bases, the helix containing the 3′ portion of the bulged strand (helix III) is displaced relative to the other helices, whereas unpaired guanines are accommodated at the branch point by the repositioning of the helix containing the 5′ portion of the bulged strand (helix II). In all cases, the relative orientation of the two helices not containing the bulged strand is not significantly affected by the unpaired bases.

The advantages of the time-resolved FRET methodology adopted in the present study are immediately apparent when we come to consider the conformational heterogeneity of the three-way junction. The existence of heterogeneity in the interarm distances in the three-way DNA junction is immediately implied by the failure to fit the donor decay profiles in terms a single D−A distance. In principle, this heterogeneity could arise from structural polymorphism, due to the existence of a small number of unique conformations of the three-way junction, or it may reflect isotropic flexibility of the junction structure, as assumed in the continuous Gaussian distance distribution model. The simplest model of structural polymorphism is a simple isomerism between two conformers. In this case, the D−A distance in each labeled junction could assume two discrete values. In fact, an energy transfer model based on two discrete D−A distances was found to provide a satisfactory fit to some of the donor decays. However, it was not possible to achieve a self-consistent analysis of all three interarm distances in the perfect junction or in any of the bulged junctions with such a model. In contrast, a Gaussian distribution of D−A distances gave excellent fits in all cases, suggesting that the conformational heterogeneity in both the perfect and bulged junctions arises from isotropic flexibility.

The three-way DNA junction appears to be uniformly flexible with respect to changes in the branch angles between helices, since the three interarm distance distributions have similar widths. This is consistent with the results of enzymatic ligation experiments involving three-way junctions. Ligation of three-way DNA junctions having sticky ends on any two of the arms produces a mixture of cyclic trimers, tetramers, and higher multimers, indicating that the branch angles in the three-way junction can adopt different values (Ma et al., 1986; Shlyakhtenko et al., 1994a). In contrast, the bulged junctions exhibit additional flexibility that is associated with only one of the three helices. This is the same helix that undergoes the greatest change in its mean position upon insertion of bulges at the branch point of the junction (helix III in the case of thymine, cytosine and adenine bulges; helix II in the case of the guanine bulge). Thus, bulges appear to introduce a point of flexibility into the structure of the three-way junction, resulting in increased mobility of one of the helices flanking the bulge site. This conclusion is in accord with enzymatic ligation experiments with bulged three-way DNA junctions, which also indicate that one of the helices flanking the bulge site has high mobility (Shlyakhtenko et al., 1994b). The enhanced flexibility of the bulged junctions is not unexpected, given that the addition of two unpaired bases to strand 2 introduces 12 extra bonds into the polynucleotide backbone at the point of connection between helices II and III. What is surprising is that this additional flexibility is only manifested in one of the helices flanking the bulge, either helix II or helix III, depending on the nature of the unpaired bases.

Conformational flexibility in three-way junctions has also been addressed in an earlier study by Shen and Hagerman (1994). These authors examined the overall structure of the central three-helix junction of a 5S ribosomal RNA using a combination of gel electrophoresis and transient electric birefringence methods. This junction is comprised of three helices (I, II, and V) bounding a central loop of unpaired nucleotides. The relative orientations of the three helices were determined by transient birefringence measurements employing a set of RNA molecules in which the helices were extended, pairwise, by 70 bp. The birefringence decay curve is sensitive to the magnitude of the permanent bend angle enclosed by the extended helices, as well as to any flexibility in this angle. The results indicated that helices I and V were almost colinear, while helix II was free to reorient with respect to the I−V axis. Since helix II flanks a loop of five unpaired nucleotides, these results are analagous to the findings of the present study of bulged three-way DNA junctions, in which one of the helices flanking the bulge also exhibits high mobility. However, Shen and Hagerman concluded that the conformational heterogeneity of helix II was due to an equilibrium between two distinct conformers, which differ in the orientation of helix II relative to the I−V axis, rather than a continuous distribution of conformers. In contrast, we found that the conformational heterogeneity in each of the bulged DNA junctions we examined was better described in terms of a continuous range of distances, or angles, between the flanking helix and the remainder of the molecule. These differences may reflect the intrinsic conformational properties of three-way junctions formed in DNA and RNA.

An interesting aspect of our study of bulged three-way DNA junctions is the finding that the change in the overall structure and conformational flexibility of these complexes is largely manifested in only one of the helices flanking the bulge site. Moreover, the nature of the unpaired bases dictates which of the flanking helices is affected. The reason for the specific effect of bulges on only one of the flanking helices, and for the singular behavior of guanine bulges, is not immediately obvious from the junction sequence. The local sequence of helices II and III around the branch point are very similar (Chart 1). However, the two sides of the junction may actually be inequivalent because of the overall three-dimensional structure of the complex. In addition, the base specificity may reflect the conformational preferences of particular bulged nucleotides. Studies of bulged DNA duplexes indicate that unpaired bases can either stack into the helix or adopt an extrahelical conformation [reviewed by Turner (1994)]. A high-resolution structural model of a bulged three-way DNA junction containing two unpaired pyrimidine bases has been determined by NMR spectroscopy

(Ouporov & Leontis, 1994). The structure shows that the two pyrimidines are extrahelical and largely exposed to solution. A related bulged junction containing two unpaired cytosine bases has also been studied in detail by NMR methods, and it was concluded that one of the bulged cytosines was extrahelical (Rosen & Patel, 1993a). Thus, it is not surprising that unpaired thymine and cytosine bases produce similar changes in the overall geometry and flexibility of the three-way junction examined here.

We also found that unpaired adenine bases affect the overall structure and flexibility of the three-way DNA junction in a manner similar to that of unpaired thymines and cytosines, suggesting that all three types of bulge adopt a similar conformation. A gel electrophoretic study of a bulged three-way DNA junction having a sequence closely related to that studied here also shows that unpaired adenine and thymine bases produce similar changes in the overall geometry of the junction (Zhong et al., 1994). However, Rosen and Patel (1993a) concluded on the basis of their NMR data that unpaired adenine bases behave differently to unpaired cytosines, being at least partly stacked into the core of the three-way junction. However, the bulged junction examined by Rosen and Patel has a sequence different from those studied here, and it is possible that the conformation of adenine bulges depends on their immediate sequence context.

Our results indicate that unpaired guanine residues produce different changes in the overall structure and flexibility of the three-way junction than do the other bulges. The guanine bulge alters the average position and mobility of helix II, while the other bulges only affect helix III. There does not appear to have been any previous study of the conformation of unpaired guanine bases in three-way DNA junctions. Our data suggest that unpaired guanine bases may adopt a different conformation in the three-way junction than the other bulges. For example, it is possible that one or both of the unpaired guanines insert into the junction core and make specific interactions with the flanking bases. The present bulged junctions would appear to be interesting candidates for more detailed structural studies.

In a previous study, time-resolved FRET was used to analyze the overall geometry and flexibility of a four-way DNA junction (Eis & Millar, 1993). It is interesting to compare the properties of three-way and four-way DNA junctions revealed by time-resolved FRET. In the four-way DNA junction, pairs of helical arms are coaxially stacked to form two continuous helical domains. The two domains are crossed at an acute angle to form an overall X shape structure (Murchie et al., 1989). The time-resolved FRET data for the four-way DNA junction revealed that the stacking domains were relatively rigid, whereas the distances across the short side of the X structure were much more heterogeneous (fwhm = 30 Å), indicating a variable angle between domains. In contrast, the FRET data for the three-way DNA junction without added bases reveal a uniformly flexible structure, with a similar range of distances between each pair of helices (Table 1). Nevertheless, the distance distributions in the perfect three-way junction are narrower than those resulting from rotations of the stacking domains in the four-way junction. However, the addition of unpaired bases at the branch point of the three-way junction introduces additional flexibility into the structure, manifested in the high mobility of one of the helices. The distance distributions involving this helix in the bulged junctions are comparable in width to the broadest distributions observed in the four-way DNA junction.

REFERENCES

Bevington, P. R. (1969) *Data Reduction and Error Analysis for the Physical Sciences*, McGraw-Hill, New York.

Cardullo, R. A., Agrawal, S., Flores, C., Zamecnik, P. C., & Wolf, D. E. (1988) *Proc. Natl. Acad. Sci. U.S.A. 85*, 8790−8794.

Clegg, R. M., Murchie, A. I. H., Zechel, A., Carlberg, C., Diekmann, S., & Lilley, D. M. J. (1992) *Biochemistry 31*, 4846−4856.

Clegg, R. M., Murchie, A. I. H., Zechel, A., & Lilley, D. M. J. (1993) *Proc. Natl. Acad. Sci. U.S.A. 90*, 2994−2998.

Cooper, J. P., & Hagerman, P. J. (1990) *Biochemistry 29*, 9261−9268.

Duckett, D. R., & Lilley, D. M. J. (1990) *EMBO J. 9*, 1659−1664.

Eis, P. S., & Millar, D. P. (1993) *Biochemistry 32*, 13852−13860.

Förster, T. (1949) *Z. Naturforsch. A 4*, 321−327.

Ghosh, S., Eis, P. S., Blumeyer, K., Fearon, K., & Millar, D. P. (1994) *Nucleic Acids Res. 22*, 3155−3159.

Gohlke, C., Murchie, A. I. H., Lilley, D. M. J., & Clegg, R. M. (1994) *Proc. Natl. Acad. Sci. U.S.A. 91*, 11660−11664.

Guo, Q., Lu, M., Seeman, N. C., & Kallenbach, N. R. (1990) *Biochemistry 29*, 570−578.

Haas, E., Katchalski-Katzir, E., & Steinberg, I. Z. (1978) *Biochemistry 17*, 5064−5070.

Hochstrasser, R. A., Chen, S.-M., & Millar, D. P. (1992) *Biophys. Chem. 45*, 133−141.

Holliday, R. (1964) *Genet. Res. 5*, 282−304.

Jensch, F., & Kemper, B. (1986) *EMBO J. 5*, 181−189.

Leontis, N. B., Kwok, W., & Newman, J. S. (1991) *Nucleic Acids Res. 19*, 759−766.

Leontis, N. B., Hills, M. T., Piotto, M., Ouporov, I. V., Malhotra, A., & Gorenstein, D. G. (1994) *Biophys. J. 68*, 251−265.

Lilley, D. M. J., & Clegg, R. M. (1993) *Annu. Rev. Biophys. Biomol. Struct. 22*, 299−328.

Liu, B., Leontis, N. B., & Seeman, N. C. (1995) *Nanobiology 3*, 177−188.

Lu, M, Guo, Q., & Kallenbach, N. R. (1991) *Biochemistry 30*, 5815−5820.

Ma, R.-I., Kallenbach, N. R., Sheardy, R. D., Petrillo, M. L., & Seeman, N. C. (1986) *Nucleic Acids Res. 14*, 9745−9753.

Messelson, M. S., & Radding, C. M. (1975) *Proc. Natl. Acad. Sci. U.S.A. 72*, 358−361.

Minigawa, T., Murakami, A., Ryo, Y., & Yamagashi, H. (1983) *Virology 126*, 183−293.

Morrison, L. E., & Stols, L. M. (1993) *Biochemistry 32*, 3095−3104.

Murchie, A. I. H., Clegg, R. M., von Kitzing, E., Duckett, D. R., Diekmann, S., & Lilley, D. M. J. (1989) *Nature 341*, 763−766.

Orr-Weaver, T. L., Szostack, J. W., & Rothstein, R. J. (1981) *Proc. Natl. Acad. Sci. U.S.A. 78*, 6354−6358.

Ouporov, I. V., & Leontis, N. B. (1995) *Biophys. J. 68*, 266−274.

Parkhurst, K. M., & Parkhurst, L. J. (1995) *Biochemistry 34*, 293−300.

Rosen, M. A., & Patel, D. J. (1993a) *Biochemistry 32*, 6563−6575.

Rosen, M. A., & Patel, D. J. (1993b) *Biochemistry 32*, 6576−6587.

Seeman, N. C., & Kallenbach, N. R. (1994) *Annu. Rev. Biophys. Biomol. Struct. 23*, 53−86.

Shen, Z., & Hagerman, P. J. (1994) *J. Mol. Biol. 241*, 415−430.

Shlyakhtenko, L. S., Rekesh, D., Lindsay, S. M., Kutyavin, I., Appella, E., Harrington, R. E., & Lyubchenko, Y. L. (1994a) *J. Biomol. Struct., & Dyn. 11*, 1175−1189.

Shlyakhtenko, L. S., Appella, E., Harrington, R. E., Kutyavin, I., & Lyubchenko, Y. L. (1994b) *J. Biomol. Struct. Dyn. 12*, 131−143.

Turner, D. H. (1992) *Curr. Opin. in Struct. Biol. 2*, 334−337.

Tuschl, T., Gohlke, C., Jovin, T. M., Westhof, E., & Eckstein, F. (1994) *Science 266*, 785−789.

Welch, J. B., Duckett, D. R., & Lilley, D. M. J. (1993) *Nucleic Acids Res. 21*, 4548−4555.

Yang, M., Ghosh, S., & Millar, D. P. (1994) *Biochemistry 33*, 15329−15337.

Zhong, M., Rashes, M. S., Leontis, N. B., & Kallenbach, N. R. (1994) *Biochemistry 33*, 3660−3667.

BI952892Z